Towards All-digital mmWave Massive MIMO: Designing around Nonlinearities

Mohammed Abdelghany, Ali A. Farid, Upamanyu Madhow, *Fellow, IEEE*, and Mark J. W. Rodwell, *Fellow, IEEE*.

***Abstract*— The small carrier wavelengths at mmWave frequencies enable a large number of antenna elements to be packed into a relatively small form factor. While existing implementations employ RF beamforming, it is now becoming possible to realize fully digital beamforming, with each antenna interfaced to a separate RF chain. This opens up the possibility of supporting multiuser MIMO, with the number of simultaneous users scales linearly with the number of antenna elements.**

In this paper, we investigate the impact of two fundamental hardware challenges in supporting such a fully digital architecture: the large bandwidth limits the available precision of analog-to-digital conversion, and the massive number of RF chains at mmWave frequencies constrains area and power consumption, which motivates relaxing the specifications on RF nonlinearities such as the IIP3. We provide guidelines on ADC precision and RF specifications for a multiuser MIMO uplink using a linear MMSE receiver, with nominal parameters corresponding to outdoor picocells operating at a data rate of 10 Gbps per user, and a carrier frequency of 140 GHz. Specifically, in nonlinearity-limited scenarios, we show that the output SNR of a user is proportional directly to the intrinsic SNR due to the nonlinearity self-noise and inversely to the system load factor.

Keywords*—*All-digital massive MIMO Uplink design, LoS channel, Nonlinearity (IIP3), low-precision ADC, Load Factor, LMMSE.

I. Introduction

Advances in silicon-based Radio Frequency Integrated Circuits (RFICs) are expected to enable next-generation communication systems to exploit the vast amounts of spectrum in the millimeter wave (mmWave) bands. The small carrier wavelengths enable the implementation of antenna arrays with a large number of elements in compact form factors. In this paper, we consider a mmWave massive MIMO uplink system design using a carrier frequency of 140 GHz for small cell applications, supporting a large number of users at data rates of 10 Gbps per user, targeting ranges of up to 100 m. While early prototypes for mmWave transceivers in the 28 and 60 GHz bands employ RF or hybrid beamforming, advances in silicon will soon enable the number of RF chains to scale with the number of antennas, hence we explore an all-digital architecture, similar to those that have become the norm for existing systems at lower carrier frequencies.

M. Abdelghany A. Farid, U. Madhow, and M. Rodwell are with the Department of Electrical and Computer Engineering, University of California at Santa Barbara, Santa Barbara, CA 93106 USA (e-mail: mabdelghany@ucsb.edu; afarid@ece.ucsb.edu; madhow@ece.ucsb.edu; rodwell@ucsb.edu).

A. Massive MIMO Uplink

We consider a massive MIMO uplink with LoS channels between mobiles and base station. Let M denotes the number of simultaneous users and N denotes the number of base station antennas with $\beta = \frac{M}{N}$ termed the *load factor*. Our running example is for $N = 256$ base station antennas and β ranging from $\frac{1}{16}$ to $\frac{1}{2}$ (i.e., M ranging from 16 to 128). To see the potential of such a system, suppose that the bandwidth is 5 GHz and that each user employs QPSK modulation (with high-rate channel coding). Ignoring channel coding overhead, the data rate per user is 10 Gbps, and the aggregate throughput ranges from 0.16 to 1.28 Tbps!

We note that the link budget for such a system is realizable with low-cost silicon:

- antenna element gain covering a hemisphere is 3 dBi,
- 16-element array at the mobile gives 12 dB transmit beamforming gain, plus 12 dB power pooling gain,
- 256-element array in the base station gives 24 dB receive beamforming gain,
- noise figure for each RF chain in the base station of 7 dB,
- the thermal noise of 5GHz BW is about -77 dBm,
- and the free space path loss of an edge user at 100 m using a carrier frequency of 140 GHz is about 115 dB.

The transmit power required from each Power Amplifier (PA) at the mobile to achieve a target SNR_{edge} can now be computed as $P_{PA} = SNR_{edge}|_{dB} - 9$ dBm. For example, SNR_{edge} of about 16 dB (shown later to suffice for our system design) requires 7 dBm PA output, which is realizable in CMOS (CMOS designs of up to 11 dBm have been reported in [1]).

B. Contributions

In this paper, we investigate two potential bottlenecks in realizing this vision: Analog-to-Digital Converters (ADCs) for such high bandwidths and linear RF front ends at such high carrier frequencies, are both costly (in terms of chip area) and power-hungry. We would like, therefore, to design with the smallest number of bits of ADC precision and the highest level of RF nonlinearity (in terms of IIP3) possible; both of which boil down to the question of how much overall nonlinearity we can get away with. In this paper, we provide an analytical framework that provides quantitative design prescriptions regarding these. Specifically, the level of tolerable nonlinearity depends on the load factor β. For example, 2-3 bits of ADC precision and an IIP3 of 9 dB suffice for $\beta = \frac{1}{16}$, while $\beta = \frac{1}{2}$ requires 4-5 bits of ADC precision and an IIP3 of 16 dB.

Our technical approach begins with the observation that, even for a moderate number of simultaneous users, the input to each antenna is well modeled as a zero-mean complex Gaussian random variable. This, together with a Bussgang decomposition for the ADC and RF nonlinearities, allows us to derive a matched filter bound on the performance of a generic user, which captures the effect of self-noise generated by the nonlinearity. This is then put together with a pessimistic estimate of the noise enhancement due to linear MMSE reception (the strategy assumed here) to provide an estimate of the SINR (signal-to-interference-plus-noise ratio). Specializing this to an edge user then yields the design prescriptions required to operate at low outage probability.

C. Related Work

There is a growing body of recent work on the spectral efficiency for quantized massive MIMO. The work of [2]–[5] used a Bussgang approximation to model the DAC and ADC. In [2], the authors derived a lower bound on the achievable rate of $M \times N$ quantized MIMO system. The authors of [3] derived the asymptotic achievable rate for the downlink channel in the presence of ADC and DAC. They discovered that increasing the load factor by four times requires one more bit of the ADC and DAC. In [4], the authors proposed a channel estimation algorithm and an approximation for the achievable rate of the quantized uplink massive MIMO system. Authors of [5] proposed a channel estimation algorithm for a channel selective quantized uplink massive MIMO system that deploys OFDM. In [6], They compared digital and hybrid RF beamforming architectures for the downlink and showed that the All-digital architecture is the most area and power efficient. A detailed hardware model was used in [7] for downlink modeling.

While our analytical approach leverages Bussgang approximations for nonlinearities as in prior work [2]–[5], we are able to provide compact design prescriptions by combining the matched filter bound with estimated noise enhancement, together with averaging over the spatial distribution of users.

II. System Model

Fig. 1 shows the system model. The base station performs horizontal scanning with a 1D half-wavelength spaced N-element array. Fig. 1 shows the antenna array and the coordinate system. We constrain the field of view to $-\pi/2 + \delta\theta \leq \theta \leq \pi/2 - \delta\theta$, and choose $\delta\theta$ such that no grating lobe appears in the array radiation pattern. Each mobile is assumed to be able to perform ideal transmit beamforming towards the base station.

The mobiles are uniformly distributed inside a region bordered by a minimum and a maximum distance away from the base station, R_{min} and R_{max}, respectively. A spatial frequency $\Omega_m = 2\pi \frac{d_x}{\lambda} \sin\theta_m$ defines the angular location of the m^{th} mobile. While the mobiles are placed randomly in our simulations, we enforce a minimum separation in spatial frequency between any two mobiles in order not to incur excessive interference, arbitrarily choosing it as half the 3dB beamwidth: $\Delta\Omega_{\text{min}} = \frac{2.783}{N}$ [8]. For example, The system could schedule such mobiles in different time slots. Fig. 2 illustrates an instantiation of the mobiles distribution over the cell area and the interference between two users if a spatial matched filter is used. We assume a Line-of-Sight (LoS) channel between the base station and the mobiles with no shadowing nor fading. The channel vector for the m^{th} mobile can be written as follows:

$$\mathbf{h}_m = A_m \, [1 \; e^{j\Omega_m} \; e^{j2\Omega_m} \; \dots \; e^{j(N-1)\Omega_m}]^{\intercal}. \tag{1}$$

where $A_m^2 = \left(\frac{\lambda}{4\pi R_m}\right)^2$ depends on the radial location R_m of mobile m, using the Friis formula for path loss. In the remainder of this section, we describe the nonlinearities modeled in our design. The LMMSE receiver used in the digital backend accounts for the self-noise coming from these nonlinearities (characterized in the next section), as well as the thermal noise.

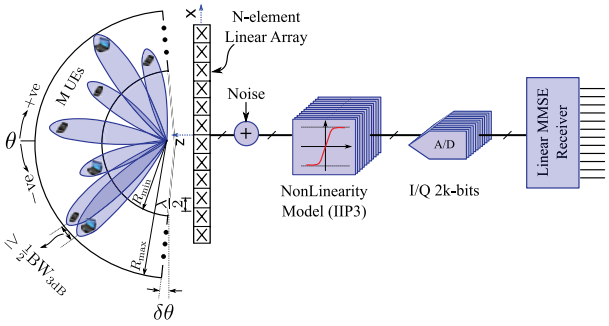

Figure 1: The figure illustrates the studied system model. The cell size is constrained radially between R_{min} and R_{max} and angularly between $-\pi/2 + \delta\theta \leq \theta \leq \pi/2 - \delta\theta$. UE and BW_{3dB} stand for the user equipment and the 3 dB beamwidth, respectively. We model the RF nonlinearity by a saturated third order polynomial model and use an overloaded uniform ADC with k-bit per dimension. A linear MMSE receiver is used after the ADCs.

A. RF Nonlinearity Model

We have reduced all amplification stages in an RF chain into one nonlinearity stage with unity gain. We model the amplitude nonlinearity distortion using a saturated third-order polynomial function, as follows,

$$y(t) = \begin{cases} x(t)(1 - \frac{4|x(t)|^2}{3 \times \text{IIP}_3}) & \text{if } |x(t)|^2 \leq \frac{\text{IIP}_3}{4} \\ \frac{x(t)}{3|x(t)|}\sqrt{\text{IIP}_3} & \text{if } |x(t)|^2 > \frac{\text{IIP}_3}{4} \end{cases} \tag{2}$$

We use the third-order Input Intercept Point (IIP3) to describe the coefficient of the third order term. IIP3 is an important design parameter for RF designers [9]. In the above formulation and without loss of generality, we assume that the average power of the input signal $\mathbb{E}(|x(t)|^2) = 0\,\text{dBm}$. Thus, we adjust the power of the input signal to be 0 dBm before it goes through the nonlinearity. Hence, the IIP3 used is called

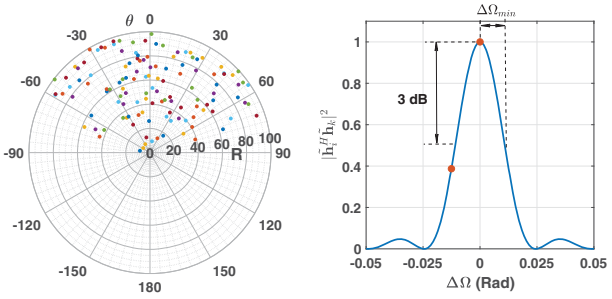

(a) (b)

Figure 2: Fig. (a) depicts an instantiation of 128 mobiles on a polar chart of cell constrained by $R_{\min} = 5m$ and $R_{\max} = 100m$ radially, and $-\pi/2 + \pi/20 \leq \theta \leq \pi/2 - \pi/20$. Fig. (b) shows the kernel of the cross-correlation of the channels of two adjacent users with a spatial frequency difference of $\Delta\Omega$, where $\tilde{\mathbf{h}}_i = \mathbf{h}_i/\sqrt{N}$. Note that the closest two users, whose relative spatial frequencies are depicted by the red points, are separated by larger or equal to half the 3dB Beamwidth.

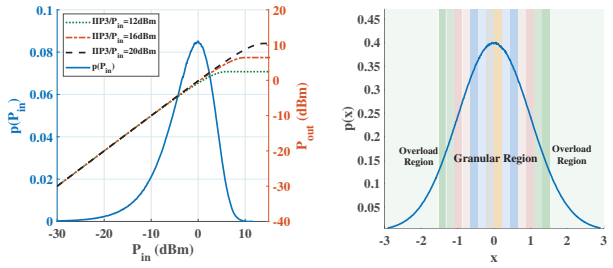

(a) (b)

Figure 3: This work studies the nonlinearity and quantization effect on the performance of a massive MIMO uplink system. Fig. (a) illustrates curves of different nonlinearity models characterized by their IIP3. It also shows the histogram of the complex envelope amplitude for a normalized-to-0dBm passband signal. Fig. (b) Illustrates the histogram of the real/imaginary parts of the normalized-to-0dBm baseband signal along with ADC quantization bins. The ADC I/O characteristic comprises the Granular and Overload regions. Highly probable small quantization errors characterize the granular region. On the other hand, low-probability large clipping errors characterize the overload region.

normalized IIP3 and is specified in dB. In this work, we consider the nonlinearity to be memoryless and free of phase distortion. Fig. 3 (a) illustrates examples of the nonlinearity model I/O characteristics.

B. ADC Model

We employ an overloaded uniform ADC [10]. It comprises two regions in its I/O characteristic, the granular and overload regions. The granular region is quantized uniformly; hence the quantization noise is bounded. On the other hand, one quantization level represents the overload region, so that the error is unbounded. Similar to the RF nonlinearity, we adjust the power of the incoming signal to be 0 dBm per dimension and design the quantizer based on that. Fig. 3 (b) depicts an example of an overloaded uniform quantizer for a standard Gaussian signal.

III. Analytical Framework

We first perform a Bussgang linearization for the received signal at each antenna element, from which we can develop a matched filter bound for the output SNR when considering only the self-noise induced by the nonlinearity. We then include the impact of thermal noise into the matched filter bound. Subsequently, we derive a lower bound for the LMMSE output SINR by using the noise enhancement for an ideal system (with no nonlinearity) as an upper bound for that in our system.

A. Bussgang linearization

For a zero mean complex random variable Z and a nonlinearity $g(\cdot)$, we can compute the best linear fit aZ (in the MMSE sense) using the orthogonality principle:

$$E[(g(Z) - aZ)Z^*] = 0,$$

so that

$$a = \frac{E[g(Z)Z^*]}{E[|Z|^2]}, \tag{3}$$

with the variance of the approximation error is given by

$$\sigma_{NL}^2 = E[|g(Z)|^2] - \frac{|E[g(Z)Z^*]|^2}{E[|Z|^2]}. \tag{4}$$

We can explicitly compute a and σ_{NL}^2 for any distribution for Z. In our case, we wish to apply this to the received signal at each antenna, which, by virtue of the central limit theorem, is well modeled as zero-mean complex Gaussian even for a moderate number of mobiles. We, therefore, compute the Bussgang linearization a and σ_{NL}^2 for a normalized setting, $Z \sim CN(0,1)$, and then scale it appropriately.

Let us now define the *intrinsic SNR* of the nonlinearity g as

$$SNR(g) = \frac{a^2}{\sigma_{NL}^2}. \tag{5}$$

Approximating the received signals at different antenna elements as jointly Gaussian, we can use Bussgang's original result [11] to infer that the error terms across the antennas are uncorrelated. We now discuss how this model can be used to get an optimistic estimate, or matched filter bound, for any given user in a multiuser MIMO system (with a large enough number of users that the preceding Gaussian model for the incoming signal at each antenna holds).

B. Matched filter bound for self-noise from nonlinearity

Suppose that $\{A_m, m = 1, \ldots, M\}$ are the amplitudes of the incoming waves for the M users. We can therefore

model the incoming signal at each receive antenna as $\tilde{Z} \sim CN(0, \sum_{m=1}^{M} A_m^2)$. Our prior analysis of nonlinearity g goes through if we scale the incoming signal to unit variance as follows,

$$Z = \frac{\tilde{Z}}{s},$$

where the scale factor s is given by

$$s^2 = MA_{rms}^2, \tag{6}$$

and

$$A_{rms} = \sqrt{\frac{1}{M}\sum_{m=1}^{M} A_m^2} \tag{7}$$

is the root mean square (rms) amplitude, averaged across users.

We, therefore, have $g(Z) = aZ + e$ as a per-antenna model for the normalized received signal. Now, when we correlate against the spatial matched filter for the m^{th} user across the N antennas, and ignore the interference from other users, we obtain the output

$$y_m = aNA_m/s + n,$$

where $\sigma_n^2 = N\sigma_{NL}^2$.

Thus, the output SNR of the matched filter for the m^{th} user is given by

$$SNR_m^{mf(g)} = \frac{a^2N^2A_m^2/s^2}{N\sigma_{NL}^2} = SNR(g)\frac{A_m^2}{\beta A_{rms}^2}, \tag{8}$$

where $\beta = \frac{M}{N}$ is the load factor. It is clear, therefore, that performance depends on the intrinsic SNR of the nonlinearity, the load factor, and the ratio of the strength of the given user compared to the average user strength.

We are interested in supporting users at the cell edge. hence we now set A_m to the worst-case amplitude A_{min}, while computing A_{rms} by a statistical average $\sqrt{\mathbb{E}[A^2]}$ given the users distribution, assuming a large enough number of users. For example, for users who are uniformly distributed over the area bounded by $[R_{min}, R_{max}]$ and a given angular range, we obtain upon straightforward computation that:

$$\frac{A_{min}^2}{A_{rms}^2} = \frac{1 - \frac{R_{min}^2}{R_{max}^2}}{2\log\frac{R_{max}}{R_{min}}}.$$

This yields that

$$SNR_{edge}^{mf(g)} = SNR(g)\ \ \frac{1}{\beta}\ \frac{1 - \frac{R_{min}^2}{R_{max}^2}}{2\log\frac{R_{max}}{R_{min}}}.$$

C. Matched filter bound with thermal noise

Suppose that σ_{th}^2 is the variance of the complex Gaussian thermal noise at each antenna. Summing up the variance of the self-noise and the thermal noise at the matched filter output, it can be shown that

$$SNR_{edge}^{mf(g+\sigma_{\text{th}}^2)} = \frac{1}{\frac{1}{SNR_{edge}^{mf(g)}} + \frac{1+SNR(g)}{SNR(g)}\frac{1}{SNR_{edge}^{mf(\sigma_{\text{th}}^2)}}}, \tag{9}$$

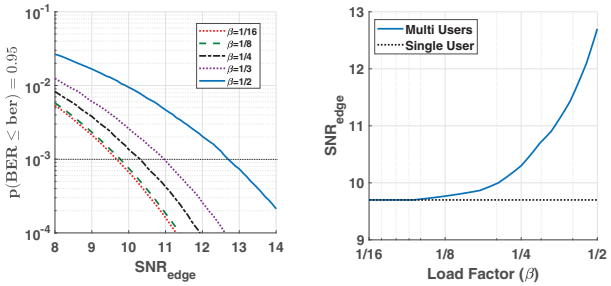

(a) (b)

Figure 4: Fig. (a) shows the BER that 95% of the UEs have better than in an ideal system, i.e., no ADC or nonlinearities, for different load factors. Fig (b) collects the SNRs of the edge user, i.e., at 100 m away from the base station, that guarantee that 95% of the mobiles have raw BER of 10^{-3} for different load factors. We use the gap in SNR between the multiuser case and single-user case in Fig. (b) to account for interference and noise enhancement when we drive a lower bound on the LMMSE output SINR.

where

$$SNR_{edge}^{mf(\sigma_{\text{th}}^2)} = \frac{NA_{min}^2}{\sigma_{\text{th}}^2}.$$

D. Lower bound on LMMSE output SINR

The effective noise variance is increased by the self-noise due to the nonlinearity, for a given user configuration. One can then show that while the output SINR for each user is larger in the ideal system, the *ratio* of the SNR to output SINR (or their difference in dB) is also larger in the ideal system. That is, the noise enhancement in the ideal system, which we denote by $SINR_{Ideal}^{Gap}$, is an upper bound on that for the actual system.

We compute this noise enhancement bound numerically by evaluating $SINR_{Ideal}^{Gap}$ through simulations, as shown in Fig. 4, where $SNR_{edge} = \frac{NA_{100m}^2}{\sigma_{\text{th}}^2}$, and A_{100m} is the received amplitude of the user at 100 m.

If we interpret LMMSE reception in the ideal system at the relatively large SNRs considered here as being close to zero-forcing reception, an intuitive approximation for the noise enhancement is given by

$$SINR_{Ideal}^{Gap} \approx 1 - \frac{M-1}{N}.$$

We find that this approximation is quite accurate in the regime considered here, but we do not at present have an analytical characterization.

IV. Numerical Results

The system parameters are as described in Sections I and II, and power control is not employed. We measure link quality by the outage probability at a target uncoded BER of 10^{-3}

Table I: This table lists the intrinsic SNR of the ADC, and the matched filter bound for an edge user (due to ADC alone) for load factors of $\frac{1}{2}$ and $\frac{1}{16}$.

k	$SNR(g)$	$\beta = 1/2, SNR_{edge}^{mf(g)}$	$\beta = 1/16, SNR_{edge}^{mf(g)}$
1	2.4 dB	-2.4 dB	6.6 dB
2	8.8 dB	4 dB	13 dB
3	14.3 dB	9.5 dB	18.5 dB
4	19.6 dB	14.8 dB	23.8 dB
5	24.9 dB	20.1 dB	29.1 dB

using QPSK. This target BER is chosen low enough for reliable performance using a high-rate channel code with relatively low decoding complexity and requires SNR of 9.7 dB for a SISO AWGN link. This now becomes our target output SINR at the output of the LMMSE receiver for an edge user.

A. Analytical Prediction

Using the noise enhancement bounds computed for the ideal system, for a target output SINR of 9.7 dB, the matched filter bound for an edge user, $SNR_{edge}^{mf(g+\sigma_{\text{th}}^2)}$, should be at least 12.7 dB and 9.7 dB for $\beta = 1/2$ and $\beta = 1/16$, respectively. We can now infer the minimum ADC precision required for these loads since the matched filter bounds must exceed the preceding targets for the corresponding nonlinearities. Table I shows intrinsic SNRs, and the corresponding matched filter bounds, for ADC alone. We conclude that ADC precision of at least 4 bits is required for $\beta = 1/2$, while a precision of 2 bits or more is required for $\beta = 1/16$. We can characterize the requirements for the RF nonlinearity similarly by cascading it with the ADC.

B. Simulation Results

We now show that simulations match our analytical predictions. Fig. 5 (a) shows the BER attained by 95% of the mobiles versus the $SNR_{edge} = \frac{NA_{100m}^2}{\sigma_{\text{th}}^2}$. Clearly, our target BER can be obtained using 4 or 5 bits of ADC precision, but not with 3 bits. A system with 4-bit ADCs requires 2 dB higher SNR (i.e., 2 dB higher transmitted power) than one with 5-bit ADCs. Fig. 5 (c) shows how the required SNR_{edge} varies with the normalized IIP3 when the RF nonlinearity is cascaded with the ADC. IIP3 of 15-16 dB is enough to be within 1dB of the performance with ADC only.

The matched filter bound in (8) clearly shows the performance degradation due to nonlinearities at high load factors. Thus, one approach to relaxing hardware specifications, both for the RF nonlinearity and the ADC, is to reduce the load factor. Figs. 5 (b) and (c) show, for example, that a 3-bit ADC with 8 dB IIP3 suffices when the load factor is reduced to $\beta = \frac{1}{16}$, with only a 1.7 dB higher requirement on transmitted power relative to an ideal system.

Table II summarizes our design prescriptions for the system considered here.

Table II: Requirements on ADC precision, IIP3, and SNR_{edge} to attain 10^{-3} of raw BER for 95% of the mobiles. SNR_{edge}^{ADC} and SNR_{edge}^{Ideal} refer to the edge SNR needed in the presence of the ADC only, and in the ideal system, respectively.

β	k	IIP3	SNR_{edge}	SNR_{edge}^{ADC}	SNR_{edge}^{Ideal}
1/2	4	16 dB	16.2 dB	15.6 dB	12.7 dB
1/2	5	15 dB	14.4 dB	13.7 dB	12.7 dB
1/16	2	9 dB	13.4 dB	12.6 dB	9.7 dB
1/16	3	8 dB	11.4 dB	10.6 dB	9.7 dB

V. Conclusions

In this paper, we have provided an analytical framework for deriving hardware specifications in all-digital mmWave massive MIMO, with design prescriptions which closely match those obtained by simulations. Our analysis shows that linearity requirements increase with the load factor. For example, 4-5 bit ADC precision with 16-15 dB of normalized IIP3 is needed for a load factor of $\beta = \frac{1}{2}$, whereas only 2-3 bits of ADC precision and 9-8 dB of normalized IIP3 are required when we reduce the load factor to $\beta = \frac{1}{16}$. The hardware designer is thus left with the following question, which can only be answered in a specific context. For a given number of simultaneous users, which is more attractive: using a moderate number of RF chains with moderate quality, or using a large number of lower-quality RF chains?

Acknowledgment

This work was supported in part by the Semiconductor Research Corporation (SRC) under the JUMP program (2018-JU-2778) and by DARPA (HR0011-18-3-0004). Use was made of the computational facilities administered by the Center for Scientific Computing at the CNSI and MRL (an NSF MRSEC; DMR-1720256) and purchased through NSF CNS-1725797. The authors thank Ahmed Ahmed and Belal Korany for the insightful discussions.

References

[1] D. Simic and P. Reynaert, "A 14.8 dbm 20.3 db power amplifier for d-band applications in 40 nm cmos," in *2018 IEEE Radio Frequency Integrated Circuits Symposium (RFIC)*. IEEE, 2018, pp. 232–235.

[2] A. Mezghani and J. A. Nossek, "Capacity lower bound of mimo channels with output quantization and correlated noise," in *IEEE International Symposium on Information Theory Proceedings (ISIT)*, 2012.

[3] J. Xu, W. Xu, and F. Gong, "On performance of quantized transceiver in multiuser massive mimo downlinks," *IEEE Wireless Communications Letters*, vol. 6, no. 5, pp. 562–565, 2017.

[4] S. Jacobsson, G. Durisi, M. Coldrey, U. Gustavsson, and C. Studer, "Throughput analysis of massive mimo uplink with low-resolution adcs," *IEEE Transactions on Wireless Communications*, vol. 16, no. 6, pp. 4038–4051, 2017.

[5] C. Studer and G. Durisi, "Quantized massive mu-mimo-ofdm uplink," *IEEE Transactions on Communications*, vol. 64, no. 6, pp. 2387–2399, 2016.

[6] H. Yan, S. Ramesh, T. Gallagher, C. Ling, and D. Cabric, "Performance, power, and area design trade-offs in millimeter-wave transmitter beamforming architectures," *arXiv preprint arXiv:1807.07201*, 2018.

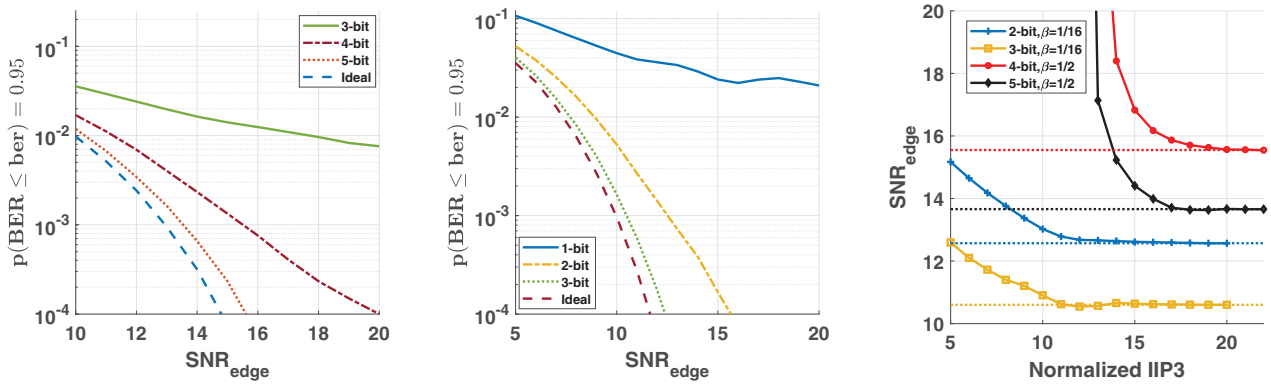

(a) (b) (c)

Figure 5: Fig (a) and (b) depict, for load factors $\frac{1}{2}$ and $\frac{1}{16}$, respectively, the BER attained by 95% of the mobiles, accounting for ADC but not RF nonlinearity. Fig (c) plots the SNR of the edge user required to guarantee that the BER target of 10^{-3} is attained by 95% of the mobiles, accounting for both RF nonlinearity and ADC.

[7] U. Gustavsson, C. Sanchéz-Perez, T. Eriksson, F. Athley, G. Durisi, P. Landin, K. Hausmair, C. Fager, and L. Svensson, "On the impact of hardware impairments on massive mimo," in *Globecom Workshops (GC Wkshps), 2014*. IEEE, 2014, pp. 294–300.

[8] C. A. Balanis, *Antenna Theory: Analysis and Design*. New York, NY, USA: Wiley-Interscience, 2005.

[9] B. Razavi and R. Behzad, *RF microelectronics*. Prentice Hall New Jersey, 1998, vol. 2.

[10] A. Gersho and R. M. Gray, *Vector quantization and signal compression*. Springer Science & Business Media, 2012, vol. 159.

[11] J. BUSSGANG, "Crosscorrelation functions of amplitude-distorted gaussian signals," *MIT Res. Lab. Elec. Tech. Rep.*, vol. 216, pp. 1–14, 1952.